International Journal of Control, Automation and Systems 16(3) (2018) 1129-1141
http://dx.doi.org/10.1007/s12555-017-0531-2
ISSN:1598-6446 eISSN:2005-4092
http://www.springer.com/12555

Adaptive Dynamic Surface Control for Spacecraft Terminal Safe Approach with Input Saturation Based on Tracking Differentiator

Guan-Qun Wu, Shen-Min Song*, and Jing-Guang Sun

Abstract: This thesis studies the spacecraft terminal safe approach control problem considering input saturation. Based on the spacecraft relative motion model and sphere collision avoidance potential function, an anti-saturation controller and an adaptive finite-time anti-saturation controller using dynamic surface control(DSC) are presented for the situations of known and unknown upper bound of external disturbances respectively, which can guarantee that no collisions happen in the tracking process. The second-order tracking differentiator is introduced to design the controllers, which avoids the differential of the virtual control signal and ensures the tracking performance of system output signals. Meanwhile, the auxiliary system is introduced to handle input saturation. Lyapunov stability theory is adopted to prove that the states of system under the designed controllers are uniformly ultimately bounded and practical finite-time stable respectively, and the chaser spacecraft can approach to the desired position without collision. The numerical simulation results demonstrate that the chaser spacecraft using the designed controllers can realize terminal safe approach to target spacecraft, which further illustrate the effectiveness of the proposed controllers.

Keywords: Collision avoidance, dynamic surface control, input saturation, potential function, terminal safe approach.

1. INTRODUCTION

With the rapid development of space technology and the increase of space strategic position, the on-orbit missions such as rendezvous and docking, space debris removal, spacecraft capture, spacecraft maintenance have caused more and more attention of many countries [1–4]. To complete the space on-orbit missions successfully, the chaser spacecraft must approach to the desired position near the target spacecraft quickly. In the complex space environment, for the further on-orbit operation, the accuracy requirement of actual arrival position must be satisfied. Thus, the terminal approach control strategy must have high control precision and strong robustness. Additionally, because the chaser is close to target in the process of terminal approach, taboo area where collision may happen easily must be avoided. Therefore, the research of spacecraft terminal approach robust control scheme considering safety constraint is the study keystone for the completion of on-orbit missions.

In recent years, many academicians have embarked on extensive researches and explorations related on control of spacecraft proximity relative motion, and many robust nonlinear control techniques have been adopted for relative motion control. For dynamic model based on the C-W equations with uncertainties, a controller for rendezvous problem with the limited-thrust was designed by handling convex optimization problem in [5]. To drive the chaser to approach to the target, a modified adaptive controller with uncertain parameters was presented in [6], under which asymptotic convergence of the system states was proved. In [7], an integral sliding mode controller was proposed using linear quadratic optimal control theory to track fuel-optimal trajectories for spacecraft hovering around elliptic orbits. Using back-stepping method and neural networks, a robust adaptive controller was designed in [8] for spacecraft rendezvous and docking, with which the system states were proved globally uniformly ultimately bounded. In [9], a neural network-based adaptive second order sliding mode controller was presented to solve relative orbital control problem. For discrete-time stochastic systems with state and disturbance dependent noise, the optimal linear state feedback control was derived under the obtained necessary condition and the sufficient condition in [10]. In [11], to eliminate the conservatism, mismatched membership functions were introduced. Also a

Manuscript received September 1, 2017; revised November 18, 2017; accepted November 30, 2017. Recommended by Associate Editor Sing Kiong Nguang under the direction of Editor Jessie (Ju H.) Park. This work was supported by the China Aerospace Science and Technology Innovation Foundation(CAST. No. JZ20160008), the State Key Program of National Natural Science Foundation of China(61333003) and the Major Program of Natural Science Foundation of China(61690210).

Guan-Qun Wu, Shen-Min Song, and Jing-Guang Sun are with the Center for Control Theory and Guidance Technology, Harbin Institute of Technology, Harbin, 150001, China (e-mails: wgqwuguanqun@163.com, songshenmin@hit.edu.cn, sunjingguanghit@163.com).
* Corresponding author.

fuzzy sampled-data controller was designed and the superiority has been verified. In [12], the optimal harvesting control and dynamics of the stochastic delay model were studied, also the performance of the theoretical results was illustrated via theoretical analysis and numerical simulations.

For the safety of the spacecraft, collision avoidance is very necessary in controller design for spacecraft proximity relative motion [13–20]. In [13], a new guidance control method based on fuzzy logic was proposed for autonomous rendezvous and docking with a non-cooperative target, which used potential function to ensure safe approaching. By using the special potential functions and a time-varying sliding manifold, the control laws were presented in [14] for maintaining configuration with avoiding obstacles. For multiple Euler-Lagrange systems, the finite-time controllers were designed to achieve accurate formation with avoiding obstacles using null-space-based and fast terminal sliding in [15, 16]. Recently, as the in-depth study on the model predictive control (MPC), some novel control schemes have been presented based on MPC for rendezvous and docking considering obstacle avoidance [17–20]. To handle spacecraft rendezvous considering obstacle avoidance and a line-of-sight cone constraint, the robust control schemes based on explicit MPC and the linear quadratic MPC with dynamically reconfigurable constraints were proposed in [17, 18]. Based on HCW model, an optimal control scheme was presented in [19], which used MPC and sequence quadratic program for rendezvous with nonlinear obstacle avoidance constraint. In [20], the linear quadratic MPC and the nonlinear MPC were applied for spacecraft rendezvous and docking, which can realize multiple obstacle avoidance.

The input of the actuator is limited in actual spacecraft relative motion control. If the input saturation is not considered in the controller design, the system control performance would be weakened, even the system instability may be caused. Therefore, input saturation should be taken into account in controller design [21–26]. In [21], the spacecraft relative motion control with obstacle avoidance was studied by using safe positively invariant sets, and a graph search algorithm was used to tackle thrust limits. In order to analyze the effect of input saturation, the auxiliary system was introduced in [22], based on which adaptive tracking controllers were designed for MIMO systems with input saturation. In [23], a dynamic surface control (DSC) scheme was presented for a class of uncertain nonlinear systems with unknown disturbance, which used a hyperbolic tangent function to approximate the input saturation. For spacecraft rendezvous and docking, an adaptive switching controller was provided in [24], which introduced an auxiliary signal to compensate effect of input saturation based on anti-windup technique. A saturated adaptive back-stepping controller for spacecraft rendezvous and proximity operations was designed in [25], which adopted auxiliary design system to deal with input saturation. In [26], the saturated function was introduced to handle input saturation constraints.

To ensure that no collisions occur in the spacecraft terminal approach, the control forces may be large to avoid the collision, which could cause that the inputs exceed the limit of the actuator. However, the literatures subject to spacecraft proximity relative motion with collision avoidance rarely consider input saturation, not to mention the consideration of the robustness of the external disturbances and finite time. These deficiencies limit practical applications of the methods. Therefore, for good engineering application, it is challenging but meaningful to design control schemes with high control precision for spacecraft terminal approach considering safe constraint and input saturation at the same time, and further the external disturbances and finite time convergence should be taken into account simultaneously.

To further research the spacecraft terminal safe approach control scheme with input saturation, sphere collision avoidance potential function is introduced to deal with taboo area in the chaser spacecraft motion, based on which two controller schemes are designed by using backstepping method and second-order tracking differentiator. Compared with some existing literatures, the main contributions of the thesis are highlighted as follows:

1) Compared with [17–20], the sphere collision avoidance potential function is introduced according to the general shape of the target spacecraft, and the sphere interior is set as taboo area, which makes collision avoidance problem in terminal approach control be simplified as boundedness problem of the reciprocal of the potential function.

2) Compared with [27], the thesis provides two effective controllers without differentiating of the virtual controls by using second-order tracking differentiator. And the adaptive law is used in second-order tracking differentiator to improve the tracking performance of the system.

3) Compared with [28], input saturation is handled by using the auxiliary system in this thesis for terminal approach considering safe constraint, which makes the designed terminal safe approach control schemes have practical significance. Further, with unknown upper bound of external disturbances, the second designed controller in the thesis can ensure safe constraint, input saturation and finite-time convergence at the same time simultaneously.

The paper is organized as follows: Firstly, a brief description of the spacecraft terminal safe approach control problem is given, including the target orbit coordinate system, spacecraft relative motion model of terminal approach, safe approach condition and related assumptions. Secondly, an anti-saturation controller and an adaptive finite-time anti-saturation controller are designed for the situations of known and unknown upper bound of external disturbances respectively. Also the corresponding

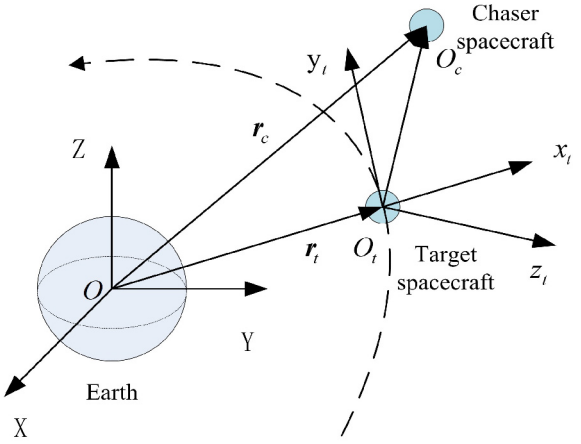

Fig. 1. Illustration of target orbit coordinate frame.

stabilities are proved and analyzed by using Lyapunov theory. Then, numerical simulations are given to verify the effectiveness of the proposed controllers. In the end, the conclusion of the thesis is presented.

2. PROBLEM FORMULATION

2.1. Spacecraft relative motion model of terminal approach

The target orbit coordinate frame $F_t(O_t x_t y_t z_t)$ is established as shown in Fig. 1: The origin of coordinate is located at the centre of target; The positive direction of y_t axis points to the target movement direction; The direction from the centre point to the target position is the positive direction of x_t axis; The positive direction of z_t axis is perpendicular to target orbital plane, which meets the right-hand rule with x_t axis and y_t axis.

The relative dynamics of the chaser and the target in earth centred inertial (ECI) frame $F_o(OXYZ)$ are described as (1) and (2) respectively:

$$\ddot{\boldsymbol{r}}_c = -\frac{\mu \boldsymbol{r}_c}{r_c^3} + \frac{\boldsymbol{f}_{dc}}{m_c} + \frac{\bar{\boldsymbol{u}}}{m_c}, \tag{1}$$

$$\ddot{\boldsymbol{r}}_t = -\frac{\mu \boldsymbol{r}_t}{r_t^3} + \frac{\boldsymbol{f}_{dt}}{m_t}, \tag{2}$$

where μ denotes the gravitational constant, $\boldsymbol{f}_{dc}$ and $\boldsymbol{f}_{dt}$ are all perturbation effects on the target and chaser, so $\boldsymbol{r}_c$ and $\boldsymbol{r}_t$ represent position vectors of the target and chaser in ECI frame $F_o(OXYZ)$, respectively. And $\ddot{\boldsymbol{r}}_c$, $\ddot{\boldsymbol{r}}_t$ are the corresponding acceleration vectors, $\bar{\boldsymbol{u}}$ is the control force of chaser, m_c and m_t are the masses of chaser and target respectively.

Relative position vector $\bar{\boldsymbol{X}}_r$ in ECI frame can be written as (3), and rewrite (1) and (2), relative acceleration vector $\ddot{\bar{\boldsymbol{X}}}_r$ can be obtained as following:

$$\bar{\boldsymbol{X}}_r = \boldsymbol{r}_c - \boldsymbol{r}_t, \tag{3}$$

$$\ddot{\bar{\boldsymbol{X}}}_r = \ddot{\boldsymbol{r}}_c - \ddot{\boldsymbol{r}}_t = -\frac{\mu \boldsymbol{r}_c}{r_c^3} + \frac{\mu \boldsymbol{r}_t}{r_t^3} + \frac{\bar{\boldsymbol{u}}}{m_c} + \frac{\boldsymbol{f}_{dc}}{m_c} - \frac{\boldsymbol{f}_{dt}}{m_t}. \tag{4}$$

Mapping (4) into $F_t(O_t x_t y_t z_t)$, yields:

$$\begin{aligned} &-\frac{\mu \boldsymbol{r}_c}{r_c^3} + \frac{\mu \boldsymbol{r}_t}{r_t^3} + \frac{\boldsymbol{u}}{m_c} + \frac{\boldsymbol{d}}{m_c} \\ &= \ddot{\boldsymbol{X}}_r + \boldsymbol{\omega}_t \times (\boldsymbol{\omega}_t \times \boldsymbol{X}_r) + \dot{\boldsymbol{\omega}}_t \times \boldsymbol{X}_r + 2\boldsymbol{\omega}_t \times \boldsymbol{X}_v, \end{aligned} \tag{5}$$

where relative position vector and the relative acceleration vector are denoted as $\boldsymbol{X}_r = [x\ y\ z]^T$ and $\ddot{\boldsymbol{X}}_r = [\ddot{x}\ \ddot{y}\ \ddot{z}]^T$, respectively. In target orbit coordinate frame, $\boldsymbol{f}_{dc} - \frac{m_c}{m_t}\boldsymbol{f}_{dt}$ and $\bar{\boldsymbol{u}}$ are expressed as disturbances $\boldsymbol{d}$ and $\boldsymbol{u}$, respectively. Let $\boldsymbol{X}_v = \dot{\boldsymbol{X}}_r$. So the position vector from earth's core to the target and the chaser can be defined as $\boldsymbol{r}_t = [r_t\ 0\ 0]^T$ and $\boldsymbol{r}_c = [x + r_t\ y\ z]^T$, respectively. The angular velocity of the target is defined as $\boldsymbol{\omega}_t = [0\ 0\ \dot{\theta}_t]^T$.

Simplifying (5), yields spacecraft terminal approach relative motion model (6)-(9) as:

$$\begin{cases} \dot{\boldsymbol{X}}_r = \boldsymbol{X}_v, \\ \dot{\boldsymbol{X}}_v = \boldsymbol{A}\boldsymbol{X}_v + \boldsymbol{B}\boldsymbol{X}_r + \boldsymbol{C} + \dfrac{\boldsymbol{d}}{m_c} + \dfrac{\boldsymbol{u}}{m_c}, \end{cases} \tag{6}$$

$$\boldsymbol{A} = 2\dot{\theta}_t \begin{bmatrix} 0 & 1 & 0 \\ -1 & 0 & 0 \\ 0 & 0 & 0 \end{bmatrix}, \tag{7}$$

$$\boldsymbol{B} = -\frac{\mu}{r_c^3}\boldsymbol{I}_{3\times 3} + \begin{bmatrix} \dot{\theta}_t^2 & \ddot{\theta}_t & 0 \\ -\ddot{\theta}_t & \dot{\theta}_t^2 & 0 \\ 0 & 0 & 0 \end{bmatrix}, \tag{8}$$

$$\boldsymbol{C} = \mu [\ \tfrac{1}{r_t^2} - \tfrac{r_t}{r_c^3}\quad 0\quad 0\ ]^T, \tag{9}$$

where $n_t = \sqrt{\frac{\mu}{a_t^3}}$, $\dot{\theta}_t = \frac{n_t(1+e_t\cos\theta_t)^2}{(1-e_t^2)^{3/2}}$, $\ddot{\theta}_t = \frac{-2n_t^2 e_t(1+e_t\cos\theta_t)^3\sin\theta_t}{(1-e_t^2)^3}$.

2.2. Safe approach condition and control objective

In the process of approaching to the target spacecraft, the chaser will be close to the target spacecraft within short distance, which may lead to collision between the chaser and the target. In order to control the chaser to arrive at the desired position around the target safely, taboo area where collisions may happen should be considered in the motion process. The thesis selects sphere interior as the taboo area whose centre is located at the centre of target, and the collision avoidance potential function is set as follows:

$$h(\boldsymbol{X}_r) = \frac{1}{R^2}\left(x^2 + y^2 + z^2 - R^2\right), \tag{10}$$

where $\boldsymbol{X}_r = [x\ y\ z]^T$, the radius of taboo area is R.

The initial position of the chaser needs to be set in safe area, that is $h(\boldsymbol{X}_{r0}) > 0$. In the process of approaching to the desired position, if the inequality $h(\boldsymbol{X}_r) > 0$ holds, the chaser moves in safe area, which means that the chaser does not collide with target in the process of approaching to the target. On the contrary, if $h(\boldsymbol{X}_r) \le 0$, the chaser is

in the taboo area where collision may happen. According to the above analysis, if $h(\boldsymbol{X}_{r0}) > 0$ is satisfied and the $1/h(\boldsymbol{X}_r)$ is bounded, the chaser can avoid collision with the target in the process of spacecraft terminal approach.

Control objective: In the thesis, two anti-saturation controllers should be designed for the spacecraft terminal approach relative motion model (6)-(9) for the situation of known and unknown upper bound of external disturbances respectively, so that the chaser using the designed controllers can approach to the desired position without collision with the target.

Remark 1: According to above analysis, the safety requirement of position can be well reflected in the value of the potential function, and collision avoidance problem can be converted into boundedness problem of reciprocal of the potential function. Thus, tracking performance and safety constraint can be considered together in control scheme, which can simplify the design of controller for terminal safe approach.

2.3. Related lemmas and assumptions

Lemma 1 [29]**:** For $n+1$ order tracking differentiator (11), if the input signal α_r contains a bounded noise $|\chi_1 - \alpha_r| \le \kappa$, there exist positive constant ν_i, $\bar{r}_i$ that make inequality (12) hold:

$$\begin{cases} \dot{\chi}_1 = -r_1 |\chi_1 - \alpha_r|^{\frac{n}{n+1}} \operatorname{sign}(\chi_1 - \alpha_r) + \chi_2, \\ \quad \cdots \\ \dot{\chi}_i = -r_i |\chi_i - \dot{\chi}_{i-1}|^{\frac{n+1-i}{n+2-i}} \operatorname{sign}(\chi_i - \dot{\chi}_{i-1}) + \chi_{i+1}, \\ \quad \cdots \\ \dot{\chi}_n = -r_n |\chi_n - \dot{\chi}_{n-1}|^{\frac{1}{2}} \operatorname{sign}(\chi_n - \dot{\chi}_{n-1}) + \chi_{n+1}, \\ \dot{\chi}_{n+1} = -r_n \operatorname{sign}(\chi_{n+1} - \dot{\chi}_n), \end{cases} \tag{11}$$

$$\begin{aligned} &|\chi_i - \alpha_{ri}| \le \nu_i \kappa^{\frac{n+2-i}{n+1}}, \quad i = 1, 2, ..., n, \\ &\left|\upsilon_j - \alpha_{r(j+1)}\right| \le \bar{r}_j \kappa^{\frac{n+1-j}{n+1}}, \quad j = 1, 2, ..., n-1, \end{aligned} \tag{12}$$

where r_i ($i = 1, 2, ..., n+1$) is positive constant, $\alpha_{r(j+1)}$ represents j order differential of α_r.

Lemma 2 [30]**:** Suppose a_1, a_2, ..., a_n are all positive constant, and ρ satisfies inequality $0 < \rho < 2$, then the following inequality holds:

$$\left(a_1^2 + a_2^2 + ... + a_n^2\right)^{\rho} \le \left(a_1^{\rho} + a_2^{\rho} + ... + a_n^{\rho}\right)^2. \tag{13}$$

Lemma 3 [31]**:** Considering the system $\dot{x} = f(x,u)$, where x is the state vector, u is input vector. There exists a Lyapunov function V, if V satisfies both of the conditions below, the system is practical finite-time stability.

1) $V$is a positive continuously differentiable function;

2) There exist $\alpha > 0$, $p \in (0,1)$, $0 < \sigma < \infty$, and an open neighborhood $U \subset U_0$ containing the origin. Also $\dot{V} \le -\alpha V^p + \sigma$ holds.

Assumption 1: The initial position and the desired position of the chaser $\boldsymbol{X}_{r0}$, $\boldsymbol{X}_{rd}$ are assumed to be set in safe area.

Assumption 2: The external disturbance $\boldsymbol{d}$ in (6) is assumed to be bounded, and satisfies the inequality $\|\boldsymbol{d}\| \le d_m$, where d_m is a positive constant.

3. CONTROLLER DESIGN

Based on the spacecraft terminal approach relative motion model (6)-(9), for the situations of known and unknown upper bound of external disturbances, an anti-saturation controller and an adaptive finite-time anti-saturation controller are presented using DSC and the second-order tracking differentiator, with which the chaser can approach to the target safely.

3.1. Anti-saturation controller design for the situation of known upper bound of external disturbances

To handle the spacecraft terminal approach relative motion model (6)-(9) with the known upper bound of external disturbances, the thesis designs an anti-saturation controller using DSC method and second-order tracking differentiator. The detailed processes of the design are as follows:

Step 1: Define the tracking error variable $\boldsymbol{z}_1$ as follows:

$$\boldsymbol{z}_1 = \boldsymbol{X}_r - \boldsymbol{X}_{rd}, \tag{14}$$

where $\boldsymbol{X}_{rd}$ is reference signal.

Compute the first order derivative of (14), yields:

$$\dot{\boldsymbol{z}}_1 = \dot{\boldsymbol{X}}_r - \dot{\boldsymbol{X}}_{rd} = \boldsymbol{X}_v - \dot{\boldsymbol{X}}_{rd}. \tag{15}$$

Define the virtual control $\boldsymbol{\alpha}_{vc1}$ as follows:

$$\boldsymbol{\alpha}_{vc1} = -k_1 \boldsymbol{z}_1, \tag{16}$$

where k_1 is a positive constant.

Step2 : To deal with input saturation, the auxiliary system (17) is introduced, where $\Delta\boldsymbol{u} = \boldsymbol{u} - \boldsymbol{u}_c$, $\boldsymbol{u}$ is the ideal control input, $\boldsymbol{u}_c$ is the actual control input.

$$\dot{\boldsymbol{\eta}} = -k_{\boldsymbol{\eta}} \eta + \frac{\Delta \boldsymbol{u}}{m_c}, \tag{17}$$

where k_η is a positive constant.

Define the tracking error variable $\boldsymbol{z}_2$ as follows:

$$\boldsymbol{z}_2 = \boldsymbol{X}_v - \dot{\boldsymbol{X}}_{rd} - \boldsymbol{\alpha}_{vc1} - \boldsymbol{\eta}. \tag{18}$$

Compute the first order derivative of (18), yields:

$$\begin{aligned} \dot{\boldsymbol{z}}_2 =& \dot{\boldsymbol{X}}_v - \ddot{\boldsymbol{X}}_{rd} - \dot{\boldsymbol{\alpha}}_{vc1} - \dot{\boldsymbol{\eta}} \\ =& \boldsymbol{A}\boldsymbol{X}_v + \boldsymbol{B}\boldsymbol{X}_r + \boldsymbol{C} + \frac{\boldsymbol{d}}{m_c} + \frac{\Delta \boldsymbol{u}}{m_c} + \frac{\boldsymbol{u}_c}{m_c} \\ & - \ddot{\boldsymbol{X}}_{rd} - \dot{\boldsymbol{\alpha}}_{vc1} + k_\eta \boldsymbol{\eta} - \frac{\Delta \boldsymbol{u}}{m_c} \end{aligned}$$

$$=\boldsymbol{AX}_v+\boldsymbol{BX}_r+\boldsymbol{C}+\frac{\boldsymbol{d}}{m_c}+\frac{\boldsymbol{u}_c}{m_c}-\ddot{\boldsymbol{X}}_{rd}-\dot{\boldsymbol{\alpha}}_{vc1}+k_\eta\boldsymbol{\eta}. \tag{19}$$

To avoid the derivative of virtual controller and improve system performance, the second-order tracking differentiator (20) is introduced in the thesis:

$$\begin{cases}\dot{\chi}_{1,i}=-r_1\left|\chi_{1,i}-\alpha_{vc1,i}\right|^{\frac{1}{2}}\operatorname{sign}\left(\chi_{1,i}-\alpha_{vc1,i}\right)+\chi_{2,i},\\ \dot{\chi}_{2,i}=-r_2\operatorname{sign}(\chi_{2,i}-\dot{\chi}_{1,i}),\end{cases} \tag{20}$$

where $i=1,2,3$, r_1 and r_2 are positive constants, define $\boldsymbol{\chi}_1$ and $\boldsymbol{\chi}_2$ as $\boldsymbol{\chi}_1=[\chi_{1,1}\ \chi_{1,2}\ \chi_{1,3}]^T$ and $\boldsymbol{\chi}_2=[\chi_{2,1}\ \chi_{2,2}\ \chi_{2,3}]^T$, respectively.

Applying Lemma 1, inequality (21) can be obtained:

$$\begin{aligned}&\left|\chi_{1,i}-\alpha_{vc1,i}\right|\le\nu_1\kappa=l_{\chi1},\\ &\left|\dot{\chi}_{1,i}-\dot{\alpha}_{vc1,i}\right|\le\bar{r}_1\kappa^{\frac{1}{2}}=l_{\chi2},\ \ i=1,2,3,\end{aligned} \tag{21}$$

where $l_{\chi1}$, $l_{\chi2}$ are positive.

For the situations that the upper bound of external disturbances is known, based on (14)-(17), the controller is designed as (22) and (23), where k_2, k_h, $\gamma_{l\chi}$, $p_{l\chi}$, $l_{\chi2c}$ are positive constants, and inequalities $k_2>\frac{1}{2}k_\eta$, $k_\eta>1$ hold, $\hat{l}_{\chi2}$ is the adaptive estimation of parameter $l_{\chi2}$.

$$\begin{aligned}\boldsymbol{u}_c=&m_c\left(-k_2\boldsymbol{z}_2-\boldsymbol{z}_1-\boldsymbol{AX}_v-\boldsymbol{BX}_r-\boldsymbol{C}+\ddot{\boldsymbol{X}}_{rd}\right)\\&+m_c\left(\dot{\boldsymbol{\chi}}_1-\hat{l}_{\chi2}\operatorname{sign}(\boldsymbol{z}_2)-\frac{d_m}{m_c}\operatorname{sign}(\boldsymbol{z}_2)-k_\eta\boldsymbol{\eta}\right)\\&+m_c\left(k_h\frac{\boldsymbol{z}_2}{\|\boldsymbol{z}_2\|^2}\left(2\dot{h}(\boldsymbol{X}_r)h^{-3}(\boldsymbol{X}_r)-h^{-2}(\boldsymbol{X}_r)\right)\right),\end{aligned} \tag{22}$$

$$\dot{\hat{l}}_{\chi2}=\gamma_{l\chi}\left(\|z_2\|_1-p_{l\chi}\left(\hat{l}_{\chi2}-l_{\chi2c}\right)\right). \tag{23}$$

Theorem 1: Consider the spacecraft terminal approach relative motion model (6)-(9) with Assumption 1 and Assumption 2, the states of the system are regulated under the designed controller (22) and adaptive law (23), the following conclusions can be drawn:

I) The variables $\boldsymbol{z}_1$, $\boldsymbol{z}_2$, $\tilde{l}_{\chi2}$, $1/h(X_r)$ are uniformly ultimately bounded.

II) The collision avoidance potential function $h(\boldsymbol{X}_r)$ is positive, that is the chaser can avoid collision with the target in the process of motion.

III) The tracking error variables $\|\boldsymbol{z}_1\|$, $\|\boldsymbol{z}_2\|$ can converge to any small neighbourhoods, that is the relative position of the chaser $\boldsymbol{X}_r$ can converge to any small range of the desired position $\boldsymbol{X}_{rd}$.

Proof: Choose the Lyapunov function candidate as

$$V_1=\frac{1}{2}\boldsymbol{z}_1^T\boldsymbol{z}_1+\frac{1}{2}\boldsymbol{z}_2^T\boldsymbol{z}_2+k_h\frac{1}{h^2(X_r)}+\frac{1}{2\gamma_\chi}\tilde{l}_{\chi2}^2, \tag{24}$$

where $\tilde{l}_{\chi2}=l_{\chi2}-\hat{l}_{\chi2}$ is the estimation error.

Compute the derivative of V_1:

$$\begin{aligned}\dot{V}_1=&\boldsymbol{z}_1^T\dot{\boldsymbol{z}}_1+\boldsymbol{z}_2^T\dot{\boldsymbol{z}}_2-2k_h\frac{\dot{h}(\boldsymbol{X}_r)}{h^3(\boldsymbol{X}_r)}-\frac{1}{\gamma_\chi}\tilde{l}_{\chi2}\dot{\hat{l}}_{\chi2}\\=&-k_1\boldsymbol{z}_1^T\boldsymbol{z}_1+\boldsymbol{z}_1^T\boldsymbol{z}_2+\boldsymbol{z}_2^T\left(\boldsymbol{AX}_v+\boldsymbol{BX}_r+\boldsymbol{C}+\frac{\boldsymbol{d}}{m_c}\right)\\&+\boldsymbol{z}_2^T\frac{\boldsymbol{u}_c}{m_c}+\boldsymbol{z}_2^T\left(-\ddot{\boldsymbol{X}}_{rd}-\dot{\boldsymbol{\alpha}}_{vc1}+k_\eta\boldsymbol{\eta}\right)\\&-2k_h\frac{\dot{h}(\boldsymbol{X}_r)}{h^3(\boldsymbol{X}_r)}-\frac{1}{\gamma_\chi}\tilde{l}_{\chi2}\dot{\hat{l}}_{\chi2}\\=&-k_1\boldsymbol{z}_1^T\boldsymbol{z}_{v1}-k_2\boldsymbol{z}_2^T\boldsymbol{z}_2+\boldsymbol{z}_2^T\left(\frac{\boldsymbol{d}}{m_c}-\frac{d_m}{m_c}\operatorname{sign}(\boldsymbol{z}_2)\right)\\&+\boldsymbol{z}_2^T\left(\dot{\boldsymbol{\chi}}_1-\hat{l}_{\chi2}\operatorname{sign}(\boldsymbol{z}_2)-\dot{\boldsymbol{\alpha}}_{vc1}\right)\\&-\frac{k_h}{h^2(\boldsymbol{X}_r)}-\frac{\tilde{l}_{\chi2}\dot{\hat{l}}_{\chi2}}{\gamma_\chi}\\\le&-k_1\boldsymbol{z}_1^T\boldsymbol{z}_{v1}-k_2\boldsymbol{z}_2^T\boldsymbol{z}_2+\frac{\|\boldsymbol{z}_2\|}{m_c}\left(\|\boldsymbol{d}\|-d_m\right)\\&+\boldsymbol{z}_2^T\left(\dot{\boldsymbol{\chi}}_1-\hat{l}_{\chi2}\operatorname{sign}(\boldsymbol{z}_2)-\dot{\boldsymbol{\alpha}}_{vc1}\right)\\&-\frac{k_h}{h^2(\boldsymbol{X}_r)}-\frac{\tilde{l}_{\chi2}\dot{\hat{l}}_{\chi2}}{\gamma_\chi}.\end{aligned} \tag{25}$$

According to (21), inequality can be derived as:

$$\begin{aligned}&\boldsymbol{z}_2^T\left(\dot{\boldsymbol{\chi}}_1-\hat{l}_{\chi2}\operatorname{sign}(\boldsymbol{z}_2)-\dot{\boldsymbol{\alpha}}_{vc1}\right)\\&=\boldsymbol{z}_2^T\dot{\boldsymbol{\chi}}_1-\hat{l}_{\chi2}\|\boldsymbol{z}_2\|_1-\sum_{i=1}^{3}z_{2,i}\dot{\alpha}_{vc1,i}\\&\le\boldsymbol{z}_2^T\dot{\boldsymbol{\chi}}_1-\hat{l}_{\chi2}\|\boldsymbol{z}_2\|_1+\sum_{i=1}^{3}z_{2,i}\left(l_{\chi2}-\dot{\chi}_{1,i}\right)\\&\le\|\boldsymbol{z}_2\|_1\left(l_{\chi2}-\hat{l}_{\chi2}\right).\end{aligned} \tag{26}$$

Substituting (26) into (25), and based on Assumption 2, (25) can be written as:

$$\begin{aligned}\dot{V}_1\le&-k_1\boldsymbol{z}_1^T\boldsymbol{z}_{v1}-k_2\boldsymbol{z}_2^T\boldsymbol{z}_2-k_h\frac{1}{h^2(\boldsymbol{X}_r)}\\&+\|\boldsymbol{z}_2\|_1\left(l_{\chi2}-\hat{l}_{\chi2}\right)-\frac{1}{\gamma_\chi}\tilde{l}_{\chi2}\dot{\hat{l}}_{\chi2}\\\le&-k_1\boldsymbol{z}_1^T\boldsymbol{z}_{v1}-k_2\boldsymbol{z}_2^T\boldsymbol{z}_2-k_h\frac{1}{h^2(\boldsymbol{X}_r)}\\&+p_{l\chi}\tilde{l}_{\chi2}\left(\hat{l}_{\chi2}-l_{\chi2c}\right).\end{aligned} \tag{27}$$

As the following inequality holds:

$$\begin{aligned}&p_{l\chi}\tilde{l}_{\chi2}\left(\hat{l}_{\chi2}-l_{\chi2c}\right)\\&=-p_{l\chi}\left(\hat{l}_{\chi2}-l_{\chi2}\right)\\&\quad\times\left(\frac{1}{2}\left(\hat{l}_{\chi2}-l_{\chi2}\right)+\frac{1}{2}\left(\hat{l}_{\chi2}+l_{\chi2}\right)-l_{\chi2c}\right)\\&=-\frac{1}{2}p_{l\chi}\left(\hat{l}_{\chi2}-l_{\chi2}\right)^2\\&\quad-\frac{1}{2}p_{l\chi}\left(\hat{l}_{\chi2}-l_{\chi2}\right)\left(\left(\hat{l}_{\chi2}+l_{\chi2}\right)-2l_{\chi2c}\right)\end{aligned}$$

$$
\begin{aligned}
&= -\frac{1}{2}p_{l\chi}\left(\hat{l}_{\chi 2}-l_{\chi 2}\right)^2 \\
&\quad +\frac{1}{2}p_{l\chi}\left(l_{\chi 2}^2-\hat{l}_{\chi 2}^2-2l_{\chi 2c}l_{\chi 2}+2l_{\chi 2c}\hat{l}_{\chi 2}\right) \\
&= -\frac{1}{2}p_{l\chi}\left(\hat{l}_{\chi 2}-l_{\chi 2}\right)^2+\frac{1}{2}p_{l\chi}\left(l_{\chi 2}^2-2l_{\chi 2c}l_{\chi 2}+l_{\chi 2c}^2\right) \\
&\quad +\frac{1}{2}p_{l\chi}\left(-l_{\chi 2c}^2-\hat{l}_{\chi 2}^2+2l_{\chi 2c}\hat{l}_{\chi 2}\right) \\
&= -\frac{1}{2}p_{l\chi}\left(\hat{l}_{\chi 2}-l_{\chi 2}\right)^2+\frac{1}{2}p_{l\chi}\left(l_{\chi 2}-l_{\chi 2c}\right)^2 \\
&\quad -\frac{1}{2}p_{l\chi}\left(\hat{l}_{\chi 2}-l_{\chi 2}\right)^2 \\
&\le -\frac{1}{2}p_{l\chi}\tilde{l}_{\chi 2}^2+\frac{1}{2}p_{l\chi}\left(l_{\chi 2}-l_{\chi 2c}\right)^2. \qquad (28)
\end{aligned}
$$

Then (27) can be further simplified as

$$
\begin{aligned}
\dot{V}_1 \le & -k_1\boldsymbol{z}_1^T\boldsymbol{z}_{v1}-k_2\boldsymbol{z}_2^T\boldsymbol{z}_2-k_h\frac{1}{h^2(\boldsymbol{X}_r)}-\frac{1}{2}p_{l\chi}\tilde{l}_{\chi 2}^2 \\
& +\frac{1}{2}p_{l\chi}\left(l_{\chi 2}-l_{\chi 2c}\right)^2 \\
\le & -\varepsilon_1 V_1+C_1, \qquad (29)
\end{aligned}
$$

where $C_1=\frac{1}{2}p_{l\chi}\left(l_{\chi 2}-l_{\chi 2c}\right)^2$, and C_1 is bounded. $\varepsilon_1=\min\left\{2k_1,2k_2,1,\gamma_{l\chi}p_{l\chi}\right\}$.

From (29), it can be seen the variables $\boldsymbol{z}_1$, $\boldsymbol{z}_2$, $\tilde{l}_{\chi 2}$, $1/h(\boldsymbol{X}_r)$ are uniformly ultimately bounded. Because $1/h(\boldsymbol{X}_r)$ is bounded and $h(\boldsymbol{X}_{r0})$ is positive, it can be concluded that $h(\boldsymbol{X}_r)\neq 0$ holds during the changes of the system states, which indicates that collision avoidance potential function $h(\boldsymbol{X}_r)$ is not equal to zero in the process of approaching to the target, that is to say the chaser moves in safe area all the time and can realize spacecraft terminal safety approach.

Therefore, conclusion I) and II) have been proved.

According (29), the following inequality holds:

$$
\dot{V}_1 \le -\left(\varepsilon_1-\frac{C_1}{V_1}\right)V_1. \qquad (30)
$$

From (30), when inequality $\varepsilon_1-\frac{C_1}{V_1}>0$ holds, it can be got that V_1 converges to compact region $V_1\le\frac{C_1}{\varepsilon_1}$. According to (24), it can be obtained $\frac{1}{2}\boldsymbol{z}_1^T\boldsymbol{z}_1$ and $\frac{1}{2}\boldsymbol{z}_2^T\boldsymbol{z}_2$ converges to compact region $\frac{1}{2}\boldsymbol{z}_1^T\boldsymbol{z}_1$, $\frac{1}{2}\boldsymbol{z}_2^T\boldsymbol{z}_2\le\frac{C_1}{\varepsilon_1}$. Further, the convergence domain of $\|\boldsymbol{z}_1\|$ and $\|\boldsymbol{z}_2\|$ is $\|\boldsymbol{z}_1\|$, $\|\boldsymbol{z}_2\|\le\sqrt{\frac{2C_1}{\varepsilon_1}}$. When ε_1 is selected large enough, the tracking error variables z_1, z_2 can converge to any small neighbourhoods.

Therefore, conclusion III) has been proved.

The proof of Theorem 1 has been completed. □

Remark 2: If $1/h(X_r)$ converges to any small neighbourhood around zero, it can be known that $h(\boldsymbol{X}_r)$ tends to infinity when $1/h(\boldsymbol{X}_r)$ tends to zero. According to this inference, the variables $\|\boldsymbol{z}_1\|$ and $\|\boldsymbol{z}_2\|$ tend to infinity, which means that the chaser moves away from the desired position. Further, it can be seen that the V_1 tends to infinity, which is in contradiction with the system stability shown in Theorem 1. Thus, on basis of the analysis above, it can be known that not the variable $1/h(\boldsymbol{X}_r)$ but the variables $\|\boldsymbol{z}_1\|$ and $\|\boldsymbol{z}_2\|$ can converge to small neighbourhoods. And because the desired position is determined, $1/h(\boldsymbol{X}_{rd})$ is bounded and positive.

Remark 3: The tracking differentiator (20) adopted for the novel DSC controller (22) can avoid the differential of the virtual control signal, at the same time, it can ensure the tracking performance of system.

Remark 4: Due to the complex external environment, the upper bound of external disturbances of the system is generally unknown, which makes the anti-saturation controller (22) be not applicable for this case. Thus, an adaptive finite-time anti-saturation controller need be proposed which is designed and analyzed in detail as following.

3.2. Adaptive finite-time anti-saturation controller design for the situation of unknown upper bound of external disturbances

To further improve the practicability of the control scheme for the system with unknown upper bound of external disturbances, the thesis further designs an adaptive finite-time anti-saturation controller.

On basis of (14)-(19) and second-order tracking differentiator, an adaptive finite-time anti-saturation controller (31) is designed, which adopts adaptive law to estimate the upper bound of unknown external disturbances, where k_2, k_h, $\gamma_{l\chi}$, $p_{l\chi}$, γ_{d1} and γ_{d2} are positive constants. Define $\mathrm{sig}(\boldsymbol{z}_1)^\gamma$ as $\mathrm{sig}(\boldsymbol{z}_1)^\gamma=\left(|z_{1,1}|^\gamma\mathrm{sign}\left(z_{1,1}\right),\ldots,|z_{1,3}|^\gamma\mathrm{sign}\left(z_{1,3}\right)\right)^T$, and the definition of $\mathrm{sig}(\boldsymbol{z}_2)^\gamma$ is similar to $\mathrm{sig}(\boldsymbol{z}_1)^\gamma$. γ is a positive constant and $0<\gamma<1$, $\hat{d}_m$ is the estimation value of upper bound of external disturbances d_m.

$$
\begin{aligned}
\boldsymbol{u}_c = & m_c\left(-k_2\boldsymbol{z}_2-\boldsymbol{z}_1-\boldsymbol{A}\boldsymbol{X}_v-\boldsymbol{B}\boldsymbol{X}_r-\boldsymbol{C}+\ddot{\boldsymbol{X}}_{rd}\right) \\
& +m_c\left(-\mathrm{sig}(\boldsymbol{z}_2)^\gamma-\frac{\boldsymbol{z}_2}{\|\boldsymbol{z}_2\|^2}\boldsymbol{z}_1^T\mathrm{sig}(\boldsymbol{z}_1)^\gamma\right) \\
& +m_c\left(\dot{\boldsymbol{\chi}}_1-\hat{l}_{\chi 2}\mathrm{sign}\left(\boldsymbol{z}_2\right)-\frac{\hat{d}_m}{m_c}\mathrm{sign}\left(\boldsymbol{z}_2\right)-k_\eta\boldsymbol{\eta}\right) \\
& +m_c\left(k_h\frac{\boldsymbol{z}_2}{\|\boldsymbol{z}_2\|^2}\left(2\dot{h}(\boldsymbol{X}_r)h^{-3}(\boldsymbol{X}_r)-h^{-(\gamma+1)}(\boldsymbol{X}_r)\right)\right), \qquad (31)
\end{aligned}
$$

$$
\dot{\hat{l}}_{\chi 2}=\gamma_{l\chi}\|\boldsymbol{z}_2\|_1-p_{l\chi}\hat{l}_{\chi 2}, \qquad (32)
$$

$$
\dot{\hat{d}}_m=\gamma_{d1}\|z_2\|-\gamma_{d2}\hat{d}_m. \qquad (33)
$$

Theorem 2: Consider the spacecraft terminal approach relative motion model (6)-(9) with Assumptions 1 and 2, for the situations of unknown upper bound of external disturbances, the states of the system are regulated under the designed adaptive controller (31) and the adaptive laws (32)-(33), the following conclusions can be drawn:

I) The states of the system are practical finite-time stable.

II) The variables z_1, z_2, $\tilde{l}_{\chi 2}$, $\tilde{d}_m$, $1/h(\boldsymbol{X}_r)$ are bounded. Further, the collision avoidance potential function $h(\boldsymbol{X}_r)$ is positive all the time, that is the chaser can avoid collision with the target in the process of motion.

III) The tracking error variables $\|z_1\|$, $\|z_2\|$ can converge to any small neighbourhoods in finite time, that is the relative position of the chaser $\boldsymbol{X}_r$ can converge to any small range of the desired position $\boldsymbol{X}_{rd}$ in finite time.

Proof: Choose the Lyapunov function candidate as

$$V_2 = \frac{1}{2}\boldsymbol{z}_1^T\boldsymbol{z}_1 + \frac{1}{2}\boldsymbol{z}_2^T\boldsymbol{z}_2 + \frac{k_h}{h^2(\boldsymbol{X}_r)} + \frac{1}{2\gamma_{l\chi}}\tilde{l}_{\chi 2}^2 + \frac{1}{2\gamma_{d1}m_c}\tilde{d}_m^2, \tag{34}$$

where $\tilde{l}_{\chi 2} = l_{\chi 2} - \hat{l}_{\chi 2}$ is the estimation error of $l_{\chi 2}$, $\tilde{d}_m = d_m - \hat{d}_m$ is the estimation error of d_m.

Compute the derivative of V_2:

$$\begin{aligned}
\dot{V}_2 =& \boldsymbol{z}_1^T\dot{\boldsymbol{z}}_1 + \boldsymbol{z}_2^T\dot{\boldsymbol{z}}_2 - k_h\frac{2\dot{h}(\boldsymbol{X}_r)}{h^3(\boldsymbol{X}_r)} - \frac{1}{\gamma_{l\chi}}\tilde{l}_{\chi 2}\dot{\hat{l}}_{\chi 2} + \frac{1}{\gamma_{d1}}\tilde{d}_m\dot{\hat{d}}_m \\
=& -k_1\boldsymbol{z}_1^T\boldsymbol{z}_1 + \boldsymbol{z}_1^T\boldsymbol{z}_2 + \boldsymbol{z}_2^T\left(\boldsymbol{A}\boldsymbol{X}_v + \boldsymbol{B}\boldsymbol{X}_r + \boldsymbol{C} + \frac{\boldsymbol{d}}{m_c}\right) \\
&+ \boldsymbol{z}_2^T\frac{\boldsymbol{u}_c}{m_c} + \boldsymbol{z}_2^T\left(-\ddot{\boldsymbol{X}}_{rd} - \dot{\boldsymbol{\alpha}}_{vc1} + k_\eta\boldsymbol{\eta}\right) \\
&- k_h\frac{2\dot{h}(\boldsymbol{X}_r)}{h^3(\boldsymbol{X}_r)} - \frac{1}{\gamma_{l\chi}}\tilde{l}_{\chi 2}\dot{\hat{l}}_{\chi 2} + \frac{1}{\gamma_{d1}}\tilde{d}_m\dot{\hat{d}}_m \\
=& -k_1\boldsymbol{z}_1^T\boldsymbol{z}_{v1} - k_2\boldsymbol{z}_2^T\boldsymbol{z}_2 - \boldsymbol{z}_2^T\mathrm{sig}(\boldsymbol{z}_2)^\gamma - \boldsymbol{z}_1^T\mathrm{sig}(\boldsymbol{z}_1)^\gamma \\
&+ \boldsymbol{z}_2^T\left(\frac{\boldsymbol{d}}{m_c} - \frac{\hat{d}_m}{m_c}\mathrm{sign}(\boldsymbol{z}_2)\right) \\
&+ \boldsymbol{z}_2^T\left(\dot{\boldsymbol{\chi}}_1 - \hat{l}_{\chi 2}\,\mathrm{sign}(\boldsymbol{z}_2) - \dot{\boldsymbol{\alpha}}_{vc1}\right) \\
&- k_h h^{-(\gamma+1)}(\boldsymbol{X}_r) - \frac{1}{\gamma_{l\chi}}\tilde{l}_{\chi 2}\dot{\hat{l}}_{\chi 2} + \frac{1}{\gamma_{d1}}\tilde{d}_m\dot{\hat{d}}_m.
\end{aligned} \tag{35}$$

As (26) and (32) hold, and inequalities $\boldsymbol{z}_1^T\mathrm{sig}(\boldsymbol{z}_1)^\gamma \geq \left(\boldsymbol{z}_1^T\boldsymbol{z}_1\right)^{\frac{\gamma+1}{2}}$, $\boldsymbol{z}_2^T\mathrm{sig}(\boldsymbol{z}_2)^\gamma \geq \left(\boldsymbol{z}_2^T\boldsymbol{z}_2\right)^{\frac{\gamma+1}{2}}$ can be obtained according to Lemma 2, equation (35) can further rewritten as:

$$\begin{aligned}
\dot{V}_2 \leq& -k_1\boldsymbol{z}_1^T\boldsymbol{z}_{v1} - k_2\boldsymbol{z}_2^T\boldsymbol{z}_2 - \left(\boldsymbol{z}_1^T\boldsymbol{z}_1\right)^{\frac{\gamma+1}{2}} - \left(z_2^T z_2\right)^{\frac{\gamma+1}{2}} \\
&- k_h\left(\frac{1}{h^2(\boldsymbol{X}_r)}\right)^{(\gamma+1)/2} + \frac{\boldsymbol{z}_2^T}{m_c}\left(\boldsymbol{d} - \hat{d}_m\,\mathrm{sign}(\boldsymbol{z}_2)\right) \\
&+ \frac{p_{l\chi}}{\gamma_{l\chi}}\tilde{l}_{\chi 2}\dot{\hat{l}}_{\chi 2} - \frac{1}{\gamma_{d1}m_c}\tilde{d}_m\dot{\hat{d}}_m.
\end{aligned} \tag{36}$$

The following inequality can be derived:

$$\begin{aligned}
\frac{\boldsymbol{z}_2^T}{m_c}\left(d - \hat{d}_m\mathrm{sign}(\boldsymbol{z}_2)\right) \leq& \frac{1}{m_c}\left(\|\boldsymbol{z}_2\|\,\|\boldsymbol{d}\| - \hat{d}_m\|\boldsymbol{z}_2\|_1\right) \\
\leq& \frac{\|\boldsymbol{z}_2\|}{m_c}\left(d_m - \hat{d}_m\right).
\end{aligned} \tag{37}$$

Substituting (37) and (33) into (36) yields

$$\begin{aligned}
\dot{V}_2 \leq& -k_1\boldsymbol{z}_1^T\boldsymbol{z}_{v1} - k_2\boldsymbol{z}_2^T\boldsymbol{z}_2 - \left(\boldsymbol{z}_1^T\boldsymbol{z}_1\right)^{\frac{\gamma+1}{2}} - \left(\boldsymbol{z}_2^T\boldsymbol{z}_2\right)^{\frac{\gamma+1}{2}} \\
&- k_h\left(\frac{1}{h^2(\boldsymbol{X}_r)}\right)^{(\gamma+1)/2} + \frac{\|\boldsymbol{z}_2\|}{m_c}\left(d_m - \hat{d}_m\right) \\
&+ \frac{p_{l\chi}}{\gamma_{l\chi}}\tilde{l}_{\chi 2}\dot{\hat{l}}_{\chi 2} - \frac{1}{\gamma_{d1}m_c}\tilde{d}_m\dot{\hat{d}}_m \\
\leq& -\left(\boldsymbol{z}_1^T\boldsymbol{z}_1\right)^{\frac{\gamma+1}{2}} - \left(\boldsymbol{z}_2^T\boldsymbol{z}_2\right)^{\frac{\gamma+1}{2}} - k_h\left(\frac{1}{h^2(\boldsymbol{X}_r)}\right)^{\frac{\gamma+1}{2}} \\
&- \left(\frac{p_{l\chi}(2\delta_2-1)}{2\gamma_{l\chi}\delta_1}\tilde{l}_{\chi 2}^2\right)^{\frac{\gamma+1}{2}} + \left(\frac{p_{l\chi}(2\delta_2-1)}{2\gamma_{l\chi}\delta_1}\tilde{l}_{\chi 2}^2\right)^{\frac{\gamma+1}{2}} \\
&+ \frac{p_{l\chi}}{\gamma_{l\chi}}\tilde{l}_{\chi 2}\dot{\hat{l}}_{\chi 2} - \left(\frac{\gamma_{d2}(2\delta_1-1)}{2\gamma_{d1}m_c\delta_1}\tilde{d}_m^2\right)^{\frac{\gamma+1}{2}} \\
&+ \left(\frac{\gamma_{d2}(2\delta_1-1)}{2\gamma_{d1}m_c\delta_1}\tilde{d}_m^2\right)^{\frac{\gamma+1}{2}} + \frac{\gamma_{d2}}{\gamma_{d1}m_c}\tilde{d}_m\dot{\hat{d}}_m.
\end{aligned} \tag{38}$$

For positive constant δ_1 satisfying $\delta_1 > \frac{1}{2}$, inequality can be derived as:

$$\begin{aligned}
\frac{\gamma_{d2}}{\gamma_{d1}m_c}\tilde{d}_m\dot{\hat{d}}_m =& \frac{\gamma_{d2}}{\gamma_{d1}m_c}\left(d_m\tilde{d}_m - \tilde{d}_m^2\right) \\
\leq& \frac{\gamma_{d2}}{\gamma_{d1}m_c}\left(-\tilde{d}_m^2 + \frac{1}{2\delta_1}\tilde{d}_m^2 + \frac{\delta_1}{2}d_m^2\right) \\
=& -\frac{\gamma_{d2}(2\delta_1-1)}{2\gamma_{d1}m_c\delta_1}\tilde{d}_m^2 + \frac{\gamma_{d2}\delta_1}{2\gamma_{d1}m_c}d_m^2.
\end{aligned} \tag{39}$$

According to [32], the inequality can be derived:

$$\left(\frac{\gamma_{d2}(2\delta_1-1)}{2\gamma_{d1}m_c\delta_1}\tilde{d}_m^2\right)^{\frac{\gamma+1}{2}} - \frac{\gamma_{d2}(2\delta_1-1)}{2\gamma_{d1}m_c\delta_1}\tilde{d}_m^2 \leq 0. \tag{40}$$

In the same way, for positive constant δ_2 satisfying$\delta_2 > \frac{1}{2}$, the following inequality holds:

$$\left(\frac{p_{l\chi}(2\delta_2-1)}{2\gamma_{l\chi}m_c\delta_1}\tilde{l}_{\chi 2}^2\right)^{\frac{\gamma+1}{2}} - \frac{p_{l\chi}(2\delta_2-1)}{2\gamma_{l\chi}m_c\delta_1}\tilde{l}_{\chi 2}^2 \leq 0. \tag{41}$$

Based on the above inequalities (39)-(41), equation (38) can be further simplified as:

$$\begin{aligned}
\dot{V}_2 \leq& -\left(\boldsymbol{z}_1^T\boldsymbol{z}_1\right)^{\frac{\gamma+1}{2}} - \left(\boldsymbol{z}_2^T\boldsymbol{z}_2\right)^{\frac{\gamma+1}{2}} - k_h\left(\frac{1}{h^2(\boldsymbol{X}_r)}\right)^{(\gamma+1)/2} \\
&- \left(\frac{p_{l\chi}(2\delta_2-1)}{2\gamma_{l\chi}\delta_1}\tilde{l}_{\chi 2}^2\right)^{\frac{\gamma+1}{2}} - \left(\frac{\gamma_{d2}(2\delta_1-1)}{2\gamma_{d1}m_c\delta_1}\tilde{d}_m^2\right)^{\frac{\gamma+1}{2}} \\
&+ \frac{\gamma_{d2}\delta_1}{2\gamma_{d1}m_c}d_m^2 + \frac{p_{l\chi}\delta_2}{2\gamma_{l\chi}}l_{\chi 2}^2 \\
\leq& -\varepsilon_2 V_2^\beta + C_2,
\end{aligned} \tag{42}$$

where $C_2 = \frac{\gamma_{d2}\delta_1}{2\gamma_{d1}m_c}d_m^2 + \frac{p_{l\chi}\delta_2}{2\gamma_{l\chi}}l_{\chi 2}^2$, and C_2 is bounded. $\varepsilon_2 = \min\left\{2^\beta, k_h^{(1-\gamma)/2}, \left(\frac{p_{l\chi}(2\delta_2-1)}{\delta_1}\right)^\beta, \left(\frac{\gamma_{d2}(2\delta_1-1)}{2\delta_1}\right)^\beta\right\}$, $\beta = \frac{\gamma+1}{2}$.

According to Lemma 3 and (42), it can be concluded that the system is practical finite-time stable, variables $\boldsymbol{z}_1$, $\boldsymbol{z}_2$, $\tilde{l}_{\chi 2}$, $\tilde{d}_m$, $1/h(\boldsymbol{X}_r)$ are bounded. Further, tracking errors $\boldsymbol{z}_1$, $\boldsymbol{z}_2$ are practical finite-time convergent.

Because $1/h(\boldsymbol{X}_r)$ is bounded and initial value $h(\boldsymbol{X}_{r0})$ is positive, it can be concluded that $h(\boldsymbol{X}_r) \neq 0$ holds during the changes of the system states, which indicates that potential function $h(\boldsymbol{X}_r)$ is not equal to zero in the process of approaching to the target, that is to say the chaser moves in safe area all the time and can realize spacecraft terminal safety approach.

Therefore, conclusion I) and II) have been proved.

According to (42), the inequality can be got:

$$\dot{V}_2 \leq -\left(\varepsilon_2 - \frac{C_2}{V_2^{\beta}}\right) V_2^{\beta}. \tag{43}$$

From (43), it can be seen that V_2 converges to compact region $V_2 \leq \left(\frac{C_2}{\varepsilon_2}\right)^{1/\beta}$. According to (34), it can be obtained that $\frac{1}{2}\boldsymbol{z}_1^T\boldsymbol{z}_1$ and $\frac{1}{2}\boldsymbol{z}_2^T\boldsymbol{z}_2$ converges to compact region $\frac{1}{2}\boldsymbol{z}_1^T\boldsymbol{z}_1, \frac{1}{2}\boldsymbol{z}_2^T\boldsymbol{z}_2 \leq \left(\frac{C_2}{\varepsilon_2}\right)^{1/\beta}$. Further, the convergence domain of $\|\boldsymbol{z}_1\|$ and $\|\boldsymbol{z}_2\|$ are $\|\boldsymbol{z}_1\|, \|\boldsymbol{z}_2\| \leq \sqrt{2}\left(\frac{C_2}{\varepsilon_2}\right)^{1/(2\beta)}$. When ε_2 is selected large enough, the tracking error variables z_1, z_2 can converge to any small neighbourhoods.

Therefore, conclusion III) has been proved.

The proof of Theorem 2 has been completed. □

Remark 5: It is worth noting that the auxiliary systems (17) can not only handle the symmetrical input saturation problem, but also can handle the asymmetric input saturation problem, which indicates that the auxiliary systems have a wider range of applications.

Remark 6: Analyzing the anti-saturation controller (22) and the adaptive finite-time anti-saturation controller (31), it can be seen that when $\boldsymbol{z}_2$ tends to zero infinitely, singularity of the closed-loop system may happen. Thus, in the simulation analysis, the controller (22) and the controller (31) are modified as (44) and (45), respectively:

$$\begin{aligned} u_c =& m_c\left(-k_2\boldsymbol{z}_2 - \boldsymbol{z}_1 - \boldsymbol{A}\boldsymbol{X}_v - \boldsymbol{B}\boldsymbol{X}_r - \boldsymbol{C} + \ddot{\boldsymbol{X}}_{rd}\right) \\ &+ m_c\left(\dot{\boldsymbol{\chi}}_1 - \hat{l}_{\chi 2}\mathrm{sign}\left(\boldsymbol{z}_2\right) - \frac{d_m}{m_c}\mathrm{sign}\left(\boldsymbol{z}_2\right) - k_\eta\boldsymbol{\eta}\right) \\ &+ m_c\left(k_h\frac{\boldsymbol{z}_2}{\|\boldsymbol{z}_2\|^2 + \Delta}\left(2\dot{h}(\boldsymbol{X}_r)h^{-3}(\boldsymbol{X}_r) - h^{-2}(\boldsymbol{X}_r)\right)\right), \end{aligned} \tag{44}$$

$$\begin{aligned} u_c =& m_c\left(-k_2\boldsymbol{z}_2 - \boldsymbol{z}_1 - \boldsymbol{A}\boldsymbol{X}_v - \boldsymbol{B}\boldsymbol{X}_r - \boldsymbol{C} + \ddot{\boldsymbol{X}}_{rd}\right) \\ &+ m_c\left(-\mathrm{sig}(\boldsymbol{z}_2)^{\gamma} - \frac{\boldsymbol{z}_2}{\|\boldsymbol{z}_2\|^2 + \Delta}\boldsymbol{z}_1^T\mathrm{sig}(\boldsymbol{z}_1)^{\gamma}\right) \\ &+ m_c\left(\dot{\boldsymbol{\chi}}_1 - \hat{l}_{\chi 2}\mathrm{sign}\left(\boldsymbol{z}_2\right) - \frac{\hat{d}_m}{m_c}\mathrm{sign}\left(\boldsymbol{z}_2\right) - k_\eta\boldsymbol{\eta}\right) \\ &+ m_c\left(\frac{k_h\boldsymbol{z}_2}{\|\boldsymbol{z}_2\|^2 + \Delta}\left(2\dot{h}(\boldsymbol{X}_r)h^{-3}(\boldsymbol{X}_r) - h^{-(\gamma+1)}(\boldsymbol{X}_r)\right)\right), \end{aligned} \tag{45}$$

where Δ is a very small positive constant.

Table 1. The parts of parameters for simulation.

Parameter	Value
The radius of the sphere in collision avoidance potential	$R = 15$ m
The maximum control force ($i = 1,2,3$)	$u_{mi} = 5$ N
The mass of the chaser	$m_c = 120$ kg
The orbital element of the target: Semi-major axis	$a = 7.0 \times 10^6$ km
The orbital element of the target: Eccentricity	$e = 0.02$
The orbital element of the target: Longitude ascending node	$\Omega = \pi/180$ rad
The orbital element of the target: Inclination	$i = 40 \times \pi/180$ rad
The orbital element of the target: Argument of perigee	$\omega = 45 \times \pi/180$ rad
The orbital element of the target: Initial true anomaly	$f = 10 \times \pi/180$ rad

4. SIMULATIONS ANALYSIS

In order to verify the effectiveness of the presented control schemes that can be used for the chaser to realize terminal safe approach, simulations are conducted in this section for the cases that the upper bound of the external disturbances is known and unknown respectively.

On basis of the parameters used in [14], parts of the parameters in the thesis are set in Table 1.

Assume that the initial values are: the relative position vector $\boldsymbol{X}_{r0} = [14 \;\; 30 \;\; -5]^T$ m, the relative speed vector $\boldsymbol{X}_{v0} = [0 \;\; 0 \;\; 0]^{\mathrm{T}}$ m/s. And the desired target position and relative speed are assumed as $\boldsymbol{X}_{rd} = [13 \;\; -19 \;\; 0]^T$ m and $\boldsymbol{X}_{vd} = [0 \;\; 0 \;\; 0]^{\mathrm{T}}$ m/s.

For the case that the upper bound of the external disturbances is known, the control parameters of the proposed controller (22) (the proposed anti-saturation controller, Proposed AC) are selected as: $k_1 = 0.005$, $k_2 = 10$, $r_1 = 0.98$, $r_2 = 0.005$, $\gamma_{l\chi} = 15$, $p_{l\chi} = 0.9$, $l_{\chi 2c} = 0.001$, $k_h = 10$, $k_\eta = 5$, $d_m = 0.02$. In order to further test the performance of the proposed controller (22), we have added a comparison with the sliding mode control (SMC) in [28]. Corresponding simulation results are shown in Figs. 2-7.

Figs. 2 and 3 depict the tracking error curves of relative position and relative velocity respectively, it can be obtained that though there are external disturbances, parameter uncertainty and input saturation of the system, the position of chaser with the proposed controller (22) can converge with small tracking error, which satisfies the requirements of the tracking performance. At the same time, the velocity of chaser can converge to a steady-state in short time. Compared with SMC, the designed controller (22) has higher control accuracy and faster convergence rate. The control force curves of the system are presented in Fig. 4. It can be seen that the control forces under the controller (22) are bounded in the whole control process. The control forces under SMC also can

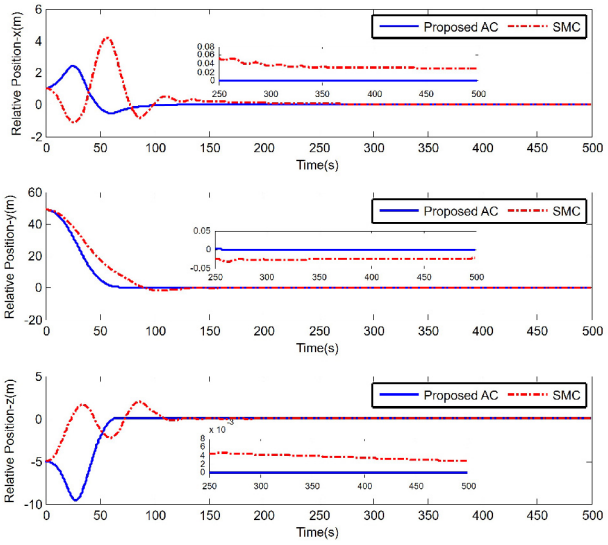

Fig. 2. The curves of relative position.

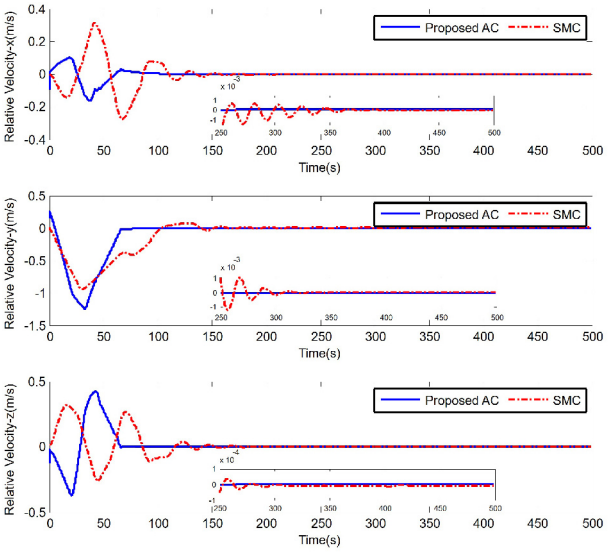

Fig. 3. The curves of relative velocity.

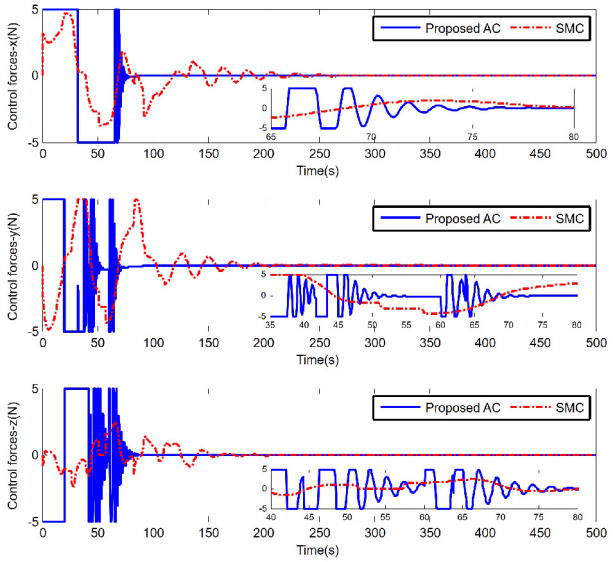

Fig. 4. The curves of control forces.

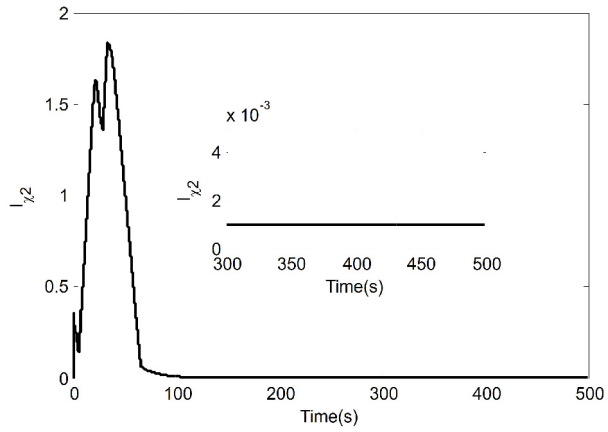

Fig. 5. The curve of $l_{\chi 2}$ under the Proposed AC.

tend to be stable after a period of time, but SMC in [28] does not have theoretical proof with regard to input saturation. Fig. 5 describes the curve of adaptive parameter $l_{\chi 2}$, which shows that the value of adaptive parameter is steady in relatively short time, indicating the effectiveness of the adaptive scheme. The curves of potential function is given in Fig. 6, from which it can be known that the value of potential function is always positive, that is to say, the chaser moves in safe area all the time during the process of approaching the desired position. To describe motion process of the chaser vividly, Fig. 7 depicts the motion trajectory of chaser in the target orbit coordinate frame. Analyzing Figs. 6 and 7, it can be obtained that the chaser has no collision with the target in the process of terminal approach under the controller (22). And the motion trajectory of chaser with the proposed controller (22) is better.

From the above, the results presented in Figs. 2-7 indicate that the chaser using the proposed controller (22) can realize the terminal safe approach effectively. Compared with SMC in [28], the designed controller (22) has higher control accuracy, faster convergence rate and more perfect theoretical proof with regard to input saturation.

For the case that the upper bound of the external disturbances is unknown, the control parameters of the proposed controller (31) (the proposed adaptive finite-time anti-saturation controller, Proposed AFAC) are selected as: $k_1 = 0.03$, $k_2 = 2$, $\gamma = 0.96$, $r_1 = 0.9$, $r_2 = 0.05$, $\gamma_{l\chi} = 0.8$, $p_{l\chi} = 0.8$, $\gamma_{d1} = 0.8$, $\gamma_{d2} = 0.3$, $k_\eta = 10$, $k_h = 2$. In order to further test the performance of the proposed controller (31), we have added a comparison with the adaptive sliding mode control (ASMC) in [28]. Corresponding simulation results are shown in Figs. 8-14.

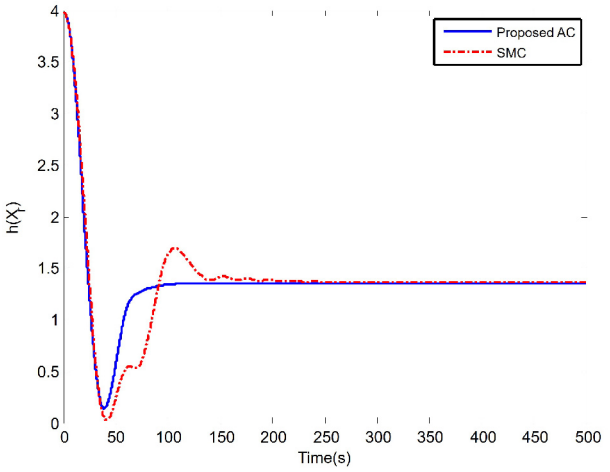

Fig. 6. The curves of potential function.

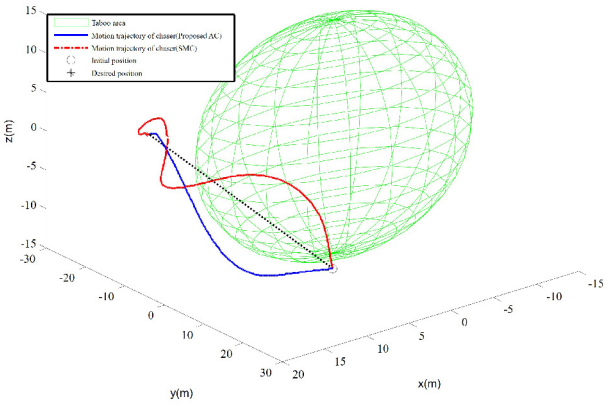

Fig. 7. The motion trajectory of chaser in target orbit coordinate frame.

The tracking error curves of relative position and relative velocity are presented in Figs. 8 and 9 respectively. The curves show that the position and the velocity of chaser with the controller (31) can converge to stable values in less than 240 seconds in spite of external disturbance, parameter uncertainty and input saturation of the system, also the position error is less than 5×10^{-4} m, indicating that the performance of system under the controller (31) satisfies the requirement of control accuracy. At the same time, the designed controller (31) has higher control accuracy and faster convergence rate compared with ASMC. Fig. 10 gives the control force curves of the system. From the control force curves, it can be seen that the control forces are limited within 5 N and tend to be stable after a period of time. But the controller (31) has more perfect theoretical proof than ASMC with regard to input saturation. On basis of Figs. 11 and 12, it can be

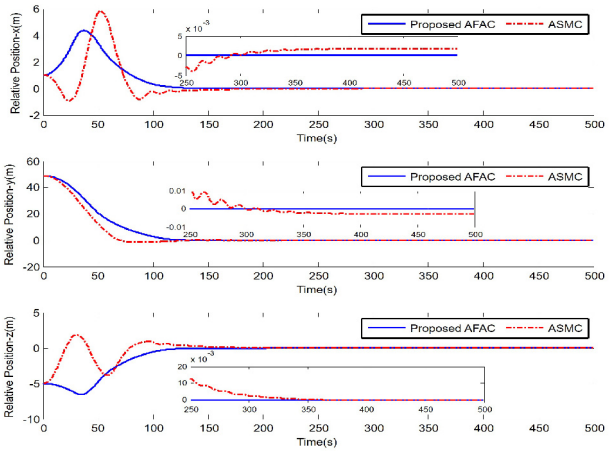

Fig. 8. The curves of relative position.

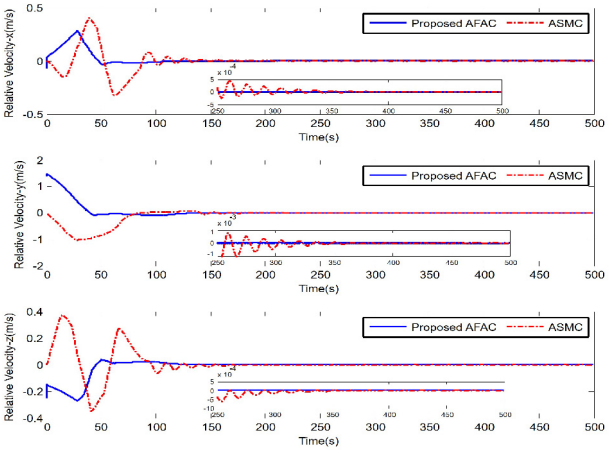

Fig. 9. The curves of relative velocity.

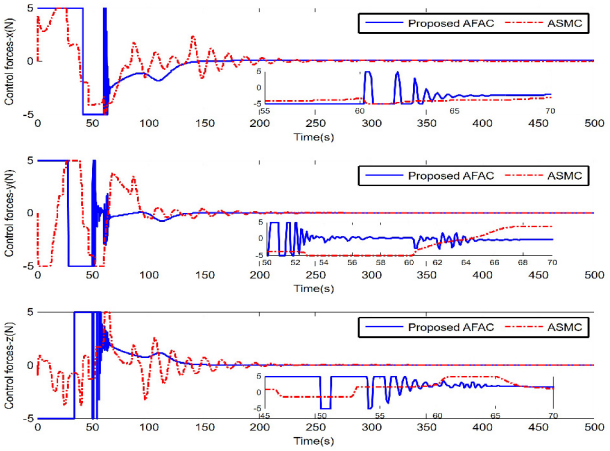

Fig. 10. The curves of control forces.

known that the estimated values $\hat{l}_{\chi 2}$ and $\hat{d}_m$ tend to maintain steady state values in limited time, which shows that

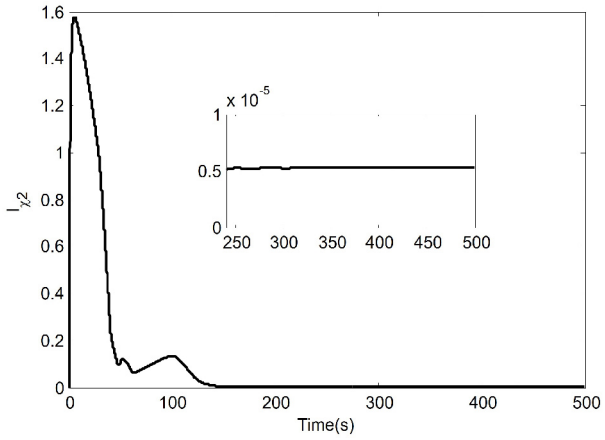

Fig. 11. The curve of $l_{\chi 2}$ under the Proposed AFAC.

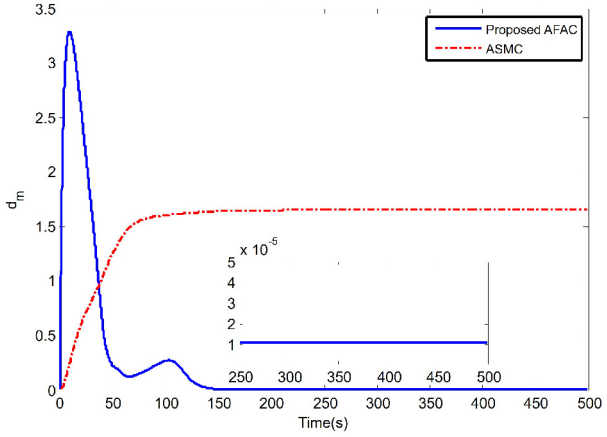

Fig. 12. The curves of d_m.

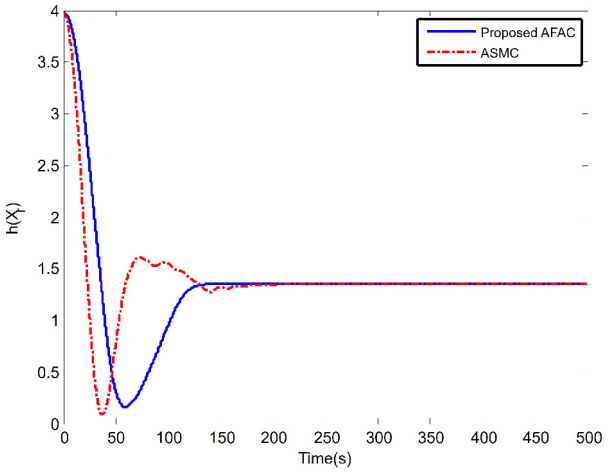

Fig. 13. The curve of potential function.

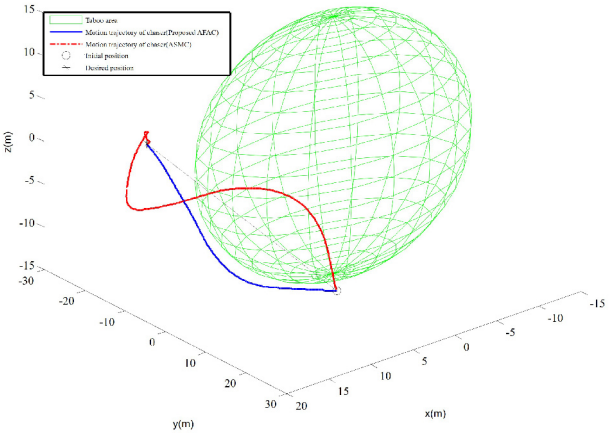

Fig. 14. The motion trajectory of chaser in target orbit coordinate frame.

the adaptive schemes are effective to estimate the values of parameter $l_{\chi 2}$and the upper bound of unknown external disturbances d_m. The value of the potential function is positive all the time as shown in Fig. 13. Fig. 14 depicts the motion trajectory of chaser in the target orbit coordinate frame. Based on Fig. 13 and Fig. 14, it can be seen that there is no collision with the target during the process of terminal approach. And the motion trajectory of chaser with the proposed controller (31) is better.

Analyzing the above simulation results presented in Figs. 8-14, it can be obtained that the chaser can realize the terminal safe approach effectively using the proposed controller(31). Compared with the convergence time, tracking errors and the curves of control forces shown in Figs. 2-4, it can be seen that the performance of the controller (31) is better than the controller (22). At the same time, the designed controller (31) has higher control accuracy, faster convergence rate and more perfect theoretical proof with regard to input saturation than ASMC in [28].

5. CONCLUSION

This thesis studies the spacecraft terminal safe approach control schemes based on DSC, auxiliary system and collision avoidance potential function. According to theoretical proofs and numerical simulation results, conclusions are drawn as follows:

1) Via introducing the sphere collision avoidance potential function, collision avoidance problem in terminal approach control is converted into boundedness problem of the reciprocal of the potential function, which can deal with safe constraint effectively and simply.

2) For the situations of known and unknown upper bound of external disturbances, an anti-saturation controller and an adaptive finite-time anti-saturation controller for spacecraft terminal safe approach are designed.

The second-order tracking differentiator is adopted to design the controllers, which avoids the differential of the virtual control signal and ensures the tracking performance of system.

3) With the two novel controllers, the states of system are uniformly ultimately bounded and practical finite-time stability respectively. And the chaser spacecraft can approach to the desired position without collision with target spacecraft. The numerical simulations further demonstrate the availability of the proposed controllers

REFERENCES

[1] C. Guariniello and D. A. DeLaurentis, "Maintenance and recycling in space: functional dependency analysis of on-orbit servicing satellites team for modular spacecraft," *AIAA SPACE 2013 Conference and Exposition*, pp. 1-16, 2013.

[2] Y. K. Ma and H. B. Ji, "Robust control for spacecraft rendezvous with disturbances and input saturation," *International Journal of Control, Automation, and Systems*, vol. 13, no. 2, pp. 353-360, 2015. [click]

[3] R. Zhong and Z. H. Zhu, "Timescale Separate Optimal control of tethered space-tug systems for space-debris Removal," *Journal of Guidance, Control, and Dynamics*, vol. 39, no. 11, pp. 2540-2545, 2016. [click]

[4] L. Sun, W. Huo, and Z. X. Jiao, "Adaptive nonlinear robust relative pose control of spacecraft autonomous rendezvous and proximity operations," *ISA transactions*, vol. 67, pp. 47-55, 2017.

[5] X. B. Yang and H. J. Gao, "Robust reliable control for autonomous spacecraft rendezvous with limited-thrust," *Aerospace Science and Technology*, vol. 24, no. 1, pp. 161-168, 2013.

[6] S. N. Wu, Z. G. Wu, G. Radice, and R. Wang, "Adaptive control for spacecraft relative translation with parametric uncertainty," *Aerospace Science and Technology*, vol. 31, no. 1, pp. 53-58, 2013.

[7] X. Huang, Y. Yan, Y. Zhou, and H. Zhang, "Sliding mode control for Lorentz-augmented spacecraft hovering around elliptic orbits," *Acta Astronautica*, vol. 103, pp. 257-268, 2014. [click]

[8] K. W. Xia, W. Huo, "Robust adaptive back-stepping neural networks control for spacecraft rendezvous and docking with uncertainties," *Nonlinear Dynamics*, vol. 84, no. 3, pp. 1683-1695, 2016.

[9] X. Huang, Y. Yan, and Y. Zhou, "Neural network-based adaptive second order sliding mode control of Lorentz-augmented spacecraft formation," *Neurocomputing*, vol. 222, pp. 191-203, 2017.

[10] X. Liu, Y. Li, and W. Zhang, "Stochastic linear quadratic optimal control with constraint for discrete-time systems," *Applied Mathematics and Computation*, vol. 228, pp. 264-270, 2014. [click]

[11] B. Wang, J. Cheng, A. Al-Barakati, and H. M. Fardoun, "A mismatched membership function approach to sampled-data stabilization for T-S fuzzy systems with time-varying delayed signals," *Signal Processing*, vol. 140, pp. 161-170, 2017.

[12] L. Liu and X. Meng, "Optimal harvesting control and dynamics of two-species stochastic model with delays," *Advances in Difference Equations*, vol. 2017, no. 1, pp. 1-17, 2017.

[13] D. W. Zhang, S. M. Song, and R. Pei, "Safe guidance for autonomous rendezvous and docking with a non-cooperative target," *Proc. of AIAA Guidance, Navigation, and Control Conference*, pp. 1-19, 2010.

[14] Q. L. Hu, H. Y. Dong, Y. M. Zhang, and G. F. Ma, "Tracking control of spacecraft formation flying with collision avoidance," *Aerospace Science and Technology*, vol. 42, pp. 353-364, 2015. [click]

[15] N. Zhou and Y. Q. Xia, "Coordination control of multiple Euler–Lagrange systems for escorting mission," *International Journal of Robust and Nonlinear Control*, vol. 25, no. 18, pp. 3596-3616, 2015. [click]

[16] J. Chen, M. Gan, J. Huang, L. Dou, and H. Fang, "Formation control of multiple Euler-Lagrange systems via null-space-based behavioral control," *Science China Information Sciences*, vol. 59, no. 1, pp. 1-11, 2016. [click]

[17] M. Leomanni, E. Rogers, and S. B. Gabriel, "Explicit model predictive control approach for low-thrust spacecraft proximity operations," *Journal of Guidance, Control, and Dynamics*, vol. 37, no. 6, pp. 1780-1790, 2014. [click]

[18] A. Weiss, M. Baldwin, R. S. Erwin, and I. Kolmanovsky, "Model predictive control for spacecraft rendezvous and docking: strategies for handling constraints and case studies," *IEEE Transactions on Control Systems Technology*, vol. 23, no. 4, pp. 1638-1647, 2015. [click]

[19] C. Jewison, R. S. Erwin, and A. Saenz-Otero, "Model predictive control with ellipsoid obstacle constraints for spacecraft rendezvous," *IFAC-Papers OnLine*, vol. 48, no. 9, pp. 257-262, 2015.

[20] H. Park, C. Zagaris, J. Virgili-Liop, R. Zappulla, I. Kolmanovsky, and M. Romano, "Analysis and experimentation of model predictive control for spacecraft rendezvous and proximity operations with multiple obstacle avoidance," *Proc. of AIAA/AAS Astrodynamics Specialist Conference*, pp, 1-17, 2016.

[21] A. Weiss, C. Petersen, M. Baldwin, R. S. Erwin, and I. Kolmanovsky, "Safe positively invariant sets for spacecraft obstacle avoidance," *Journal of Guidance, Control, and Dynamics*, vol. 38, no. 4, pp. 720-732, 2014.

[22] M. Chen, S. S. Ge, and B. B. Ren, "Adaptive tracking control of uncertain MIMO nonlinear systems with input constraints," *Automatica*, vol. 47, no. 3, pp. 452-465, 2011.

[23] M. Chen, G. Tao, and B. Jiang, "Dynamic surface control using neural networks for a class of uncertain nonlinear systems with input saturation," *IEEE Transactions on Neural Networks and Learning Systems*, vol. 26, no. 9, pp. 2086-2097, 2015.

[24] K. W. Xia and W. Huo, "Robust adaptive backstepping neural networks control for spacecraft rendezvous and docking with input saturation," *ISA transactions*, vol. 62, pp. 249-257, 2016.

[25] L. Sun, W. Huo, and Z. X. Jiao, "Adaptive backstepping control of spacecraft rendezvous and proximity operations with input saturation and full-state constraint," *IEEE Transactions on Industrial Electronics*, vol. 64, no. 1, pp. 480-492, 2017.

[26] Y. Guo, J. Guo, A. Li, and C. Wang, "Attitude Coordination Control for formation flying spacecraft based on the rotation matrix," *Journal of Aerospace Engineering*, vol. 30, no. 5, pp. 04017051, 2017.

[27] A. Imani and B. Beigzadeh, "Robust control of spacecraft rendezvous on elliptical orbits: Optimal sliding mode and back-stepping sliding mode approaches," *Proceedings of the Institution of Mechanical Engineers, Part G: Journal of Aerospace Engineering*, vol. 230, no. 10, pp. 1975-1989, 2016.

[28] X. Li and S. Song, "Slowly rotating non-cooperative target fast fly-around collision avoidance control," *Control and Decision*, doi: 10.13195/j.kzyjc.2017.0569, 2018.

[29] G. F. Sun, D. W. Li, and X. M. Ren, "Modified neural dynamic surface approach to output feedback of MIMO nonlinear systems," *IEEE Transactions on Neural Networks and Learning Systems*, vol. 26, no. 2, pp. 224-236, 2015. [click]

[30] S. H. Yu, X. H. Yu, B. Shirinzadeh, and Z. H. Man, "Continuous finite-time control for robotic manipulators with terminal sliding mode," *Automatica*, vol. 41, no. 11, pp. 1957-1964, 2005. [click]

[31] Q. L. Hu, B. Y. Jiang, and M. I. Friswell, "Robust saturated finite time output feedback attitude stabilization for rigid spacecraft," *Journal of Guidance, Control, and Dynamics*, vol. 37, no. 6, pp. 1914-1929, 2014. [click]

[32] Z. Zhu, Y. Xia, and M. Fu, "Attitude stabilization of rigid spacecraft with finite-time convergence," *International Journal of Robust and Nonlinear Control*, vol. 21, no. 6, pp. 686-702, 2011.

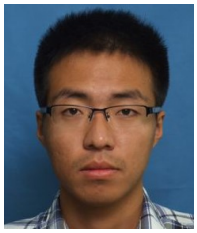

Guan-Qun Wu received his B.S. and M.S. degrees in Control Science and Engineering from Harbin Institute of Technology. Currently, he is a Ph.D. student in the School of Astronautics at the same university. His main research interests include spacecraft orbit optimization and nonlinear control.

Shen-Min Song received his Ph.D. degree in Control Theory and Application from Harbin Institute of Technology. He is currently a professor in the School of Astronautics at Harbin Institute of Technology. His main research interests include spacecraft guidance and nonlinear control.

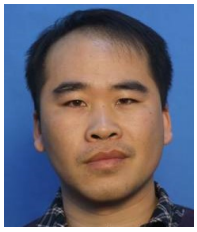

Jing-Guang Sun received his M.S. degree in School of Automation from Harbin Engineering University. Now he is a Ph.D. student in the School of Astronautics at Harbin Institute of Technology. His main research interests are hypersonic aircrafts control and nonlinear control.